

HS 1216+5032: a physical quasar pair with one radio-loud broad absorption line quasar

P. J. Green,^{1*} Thomas L. Aldcroft,¹ Warren R. Brown,¹ Olga Kuhn² and Abhijit Saha³

¹*Harvard-Smithsonian Center for Astrophysics, 60 Garden Street, Cambridge, MA 02138, USA*

²*Joint Astronomy Center, 660 N. A'ohoku Place, University Park, Hilo, HI 96720, USA*

³*Kitt Peak National Observatory, National Optical Astronomy Observatory, PO Box 26372, Tucson, AZ 85726, USA*

Accepted 2004 January 5. Received 2003 December 31; in original form 2003 October 20

ABSTRACT

We report on new multiwavelength observations of HS 1216+5032, a pair of quasi-stellar objects (QSOs) at $z = 1.45$ separated by 9.1 arcsec, which has been a perennial candidate for a massive dark lens. We explore high signal-to-noise ratio optical spectra from the MMT of both components, which show that aside from the effects of absorption, the emission-line profiles are quite similar. Near-infrared spectra from the United Kingdom Infrared Telescope show identical velocities in H α emission, but a significant difference in the strength of the narrow component, which is difficult to explain in a lens scenario. We highlight that, based on data from the Very Large Array Faint Images of the Radio Sky survey, HS 1216+5032B is a radio-loud broad absorption line QSO, which certifies HS 1216+5032 as a physical quasar pair. Intriguingly, both quasars show spectroscopic evidence for high accretion rates and large Eddington ratios L/L_{Edd} , supporting the hypothesis that close galaxy interactions trigger nuclear activity.

Key words: gravitational lensing – quasars: absorption lines – quasars: individual: HS 1216+5032 – X-rays: general – X-rays: individual: HS 1216+5032.

1 INTRODUCTION

Most gravitational lens candidates with separations $\Delta\theta < 3$ arcsec have identifiable primary lens galaxies in deep Near-Infrared Camera and Multi-Object Spectrometer (NICMOS) observations.¹ There are 16 wide separation quasar pairs (WSQPs, with $3 < \Delta\theta < 10$ arcsec), which all require large lensing masses. Three are bona fide gravitational lenses, each with similar optical/radio flux ratios, negligible spectroscopic differences, and a lens galaxy. One shows a host in the faint but not the bright NICMOS image, so could be a binary (Muñoz et al. 2001). Three more systems are pairs with strongly discrepant flux ratios, or $>3\sigma$ velocity differences, so are very probably binary quasars. The remaining nine are WSQPs with essentially identical redshifts for which no lens galaxy or cluster has been detected. If these WSQPs are gravitationally lensed, then they are produced by cluster-scale masses that failed to make substantial galaxies (i.e. ‘dark clusters’). However, without direct detection of lens baryons, proof of lensing is challenging. Detection of time delays between the light curves of lensed image components requires intensive monitoring over time-scales which may span years. The required time-scales depend strongly on lens geometries, which are unknown in the dark lens case. Direct detection of shear in the quasar

host galaxy images can serve as proof of lensing, but is also difficult (Keeton et al. 2000). It is proving easier to disprove lensing for any particular case than to prove it (Green et al. 2002; Aldcroft & Green 2003).

Of the nine potentially lensed WSQPs, we here examine the widest (9.1 arcsec) pair, HS 1216+5032, which was discovered in the Hamburg Quasar Survey (Hagen et al. 1996). The components are bright ($B_A = 17.2$ and $B_B = 19.0$), and the redshifts of the two components ($z = 1.455 \pm 0.005$) are identical within the errors. Given the wide separation of the pair, an intervening lensing cluster mass should be easily detectable (i.e. in optical or X-rays) even with an unusually low baryon fraction ($>1/3$ normal).² No lensing galaxy or cluster is evident to an imaging depth of $R \sim 22.5$ mag (Hagen et al. 1996). Nevertheless, the case for lensing was invigorated by a detailed ultraviolet (UV) spectroscopic study (Lopez, Hagen & Reimers 2000) with the *Hubble Space Telescope* (HST) Faint Object Spectrograph (FOS), which found a complex of intervening C IV absorber systems. At the $z = 0.72$ redshift of the absorber system, the minimum velocity dispersion required of an object causing the observed image separation in a standard lens

² For a singular isothermal sphere model of a lensing cluster, the minimum flux redshift is about 0.7, for which the expected X-ray flux of the lensing cluster would be $\sim 2 \times 10^{-14}$ erg cm⁻² s⁻¹, and an L^* elliptical has $R \sim 21$.

*E-mail: pgreen@cfa.harvard.edu

¹ See <http://cfa-www.harvard.edu/castles>.

model³ is only 640 km s^{-1} . The three absorbers are observed to span 1500 km s^{-1} along the line of sight, which could be taken as strong evidence for a cluster lensing potential, as noted by the authors.

HS 1216+5032 with its cluster of intervening absorbers provides a particularly interesting case for a dark lens, so we obtained optical and infrared (IR) spectroscopy to further investigate spectral differences, as described in Sections 2 and 3. We also analyse measurements from the Very Large Array (VLA) Faint Images of the Radio Sky (FIRST) survey (Section 4). In Section 5, we show that the radio data effectively rule out the lens scenario, and we briefly discuss HS 1216+5032 in the context of models for interaction-triggering of active galactic nuclei (AGN).

2 OPTICAL SPECTRA AND COLOURS

Both ground-based (Hagen et al. 1996) and *HST* FOS spectra (Lopez et al. 2000) show that only the fainter component (HS 1216+5032B) shows strong broad absorption line (BAL) systems in $\text{Ly}\alpha$, C I, C II, C III], C IV, N III, N V and O VI. This has led several authors to conclude that the pair is a true binary. However, the existence of BALs in only one quasar of a wide pair such as HS 1216+5032 may not be adequate to dismiss the lens hypothesis for several reasons. First, some spectral differences are always seen between images in lenses. The degree to which spectral similarity should be used as an argument for lensing has been a continuing subject of debate. Beyond consistent redshifts, no quantitative spectral similarity criterion has been devised to label a pair as definitely lensed or not (i.e. Falco et al. 1999; Peng et al. 1999). Secondly, the spectral differences might be explained in a lensing scenario by (1) narrow BAL wind/cloud geometry combined with viewing angles (Chelouche 2003), (2) variability (Barlow et al. 1992) and time delay, and/or (3) microlensing and dust (e.g. Lewis et al. 2002).

We obtained optical spectroscopy of the two components at the Multiple Mirror Telescope (MMT) on 2003 April 03 with the blue channel of the MMT spectrograph. We exposed for 35 min with the 300 l mm^{-1} grating centred at 6000 \AA and a 1.25 -arcsec slit, thereby achieving 2 \AA pixel^{-1} resolution. Fig. 1 shows an overplot of the flux-calibrated spectra, with the spectrum of HS 1216+5032B scaled up by a constant factor of 4. We note that strong BALs affect the emission-line profiles of HS 1216+5032B. Using the ‘balnicity index’ (BI)⁴ of Weymann et al. (1991), we measure $BI = 1870$, with maximum outflow velocity $v_{\text{max}} = 9500 \pm 1500 \text{ km s}^{-1}$ (including a conservative redshift error of ± 0.005). A revised definition from Hall et al. (2002), the absorption index (AI), yields $AI = 4178 \pm 9 \text{ km s}^{-1}$.

The $\text{Mg II } \lambda 2800$ emission line of HS 1216+5032A shows a strong ($W_{\lambda}^{\text{rest}} = 0.8 \pm 0.04 \text{ \AA}$) narrow absorption line (FWHM = $480 \pm 50 \text{ km s}^{-1}$) at very nearly the systemic redshift. For HS 1216+5032B, we identify broad shallow absorption on the blue

³ The image separation $\Delta\theta = 8\pi(\sigma_v/c)^2 D_{\text{LS}}/D_{\text{OS}}$ depends only on the velocity dispersion of the potential σ_v and the ratio of the comoving distances between the lens and the source, D_{LS} , and the observer and the source, D_{OS} . Here we assume a single isothermal sphere (SIS) model (Schneider, Ehlers & Falco 1992) and throughout use $H_0 = 70 \text{ km s}^{-1} \text{ Mpc}^{-1}$, $\Omega_M = 0.3$ and $\Omega_{\Lambda} = 0.7$.

⁴ The BI is a measure of the equivalent width of absorption measured in km s^{-1} , between 3000 and $25\,000 \text{ km s}^{-1}$ blueward of the expected systemic redshift z_{sys} of the emission line, where z_{sys} is preferably based on a low-ionization narrow emission line. The integration includes only contiguous troughs at 90 per cent of the continuum level, and spanning $>2000 \text{ km s}^{-1}$. A positive BI indicates a classic BAL. The AI is a revised calculation that admits measurements of narrower troughs, and provides for error estimates.

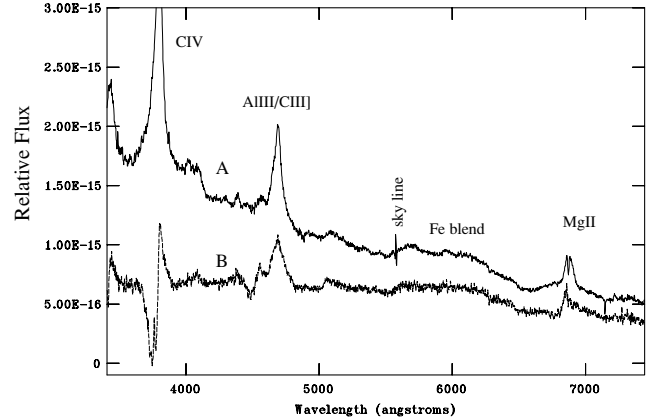


Figure 1. The optical MMT spectrum of HS 1216+5032A is shown at the top, with the spectrum of HS 1216+5032B shown at the bottom, scaled upward by a constant factor of 4 for display purposes. The continuum shapes are not reliable. Strong BALs affect the emission-line profiles of HS 1216+5032B. The $\text{Mg II } \lambda 2800$ emission line of HS 1216+5032A shows a narrow absorption line at 6871 \AA (observed). The small spike at 5577 \AA results from poor night-sky line subtraction there.

half of the $\text{Mg II } \lambda 2800$ emission line, and clear broad troughs in the A IIII/C III] complex. This is consistent with the finding that two of three BAL systems detected in the *HST* FOS spectra (-1000 , -3000 and -4000 km s^{-1} , respectively; Lopez et al. 2000) show smooth broad absorption in low-ionization lines of $\text{Ly}\alpha$, C III] $\lambda 1334$ and C III] $\lambda 977$. We measure $AI = 0$ for both troughs, so HS 1216+5032B may thus be a borderline member of the class of low-ionization BAL (loBAL) QSOs.

The component continuum slopes in Fig. 1 appear to be discrepant. Excess reddening of the BALQSO is expected if there is dust associated with the absorber, and some reddening has been demonstrated in recent samples from the Sloan Digital Sky Survey (SDSS; Reichard et al. 2003). However, we obtained the MMT spectra of both objects simultaneously, with the slit necessarily at 34° from the parallactic angle. At the mean airmass 1.14, differential atmospheric refraction would cause a 0.45 -arcsec offset between light at 3500 and 7000 \AA across the 1.25 -arcsec slit. The apparent continuum shapes may not be trustworthy, or may be due to differing line-of-sight absorption.

Because no published CCD photometry is available for the pair that might confirm the difference in optical spectral slopes, we obtained images at the WIYN 3.5-m on Kitt Peak. On 2003 June 5 using the MiniMosaic camera, we obtained two exposures of 50 s each in Harris *B* and *R* filters. We find $B_A = 17.32$ and $B_B = 19.4$, and in the red $R_A = 16.79$ and $R_B = 18.5$, with random photometric errors $<0.04 \text{ mag}$ and nightly solution errors $\sim 0.05 \text{ mag}$. The colours of the two components are $(B-R)_A = 0.52$ and $(B-R)_B = 0.90 \text{ mag}$ (both $\pm 0.05 \text{ mag}$), so they thus differ significantly, with $\Delta(B-R) = 0.37 \pm 0.06$.

While the possibility of slit losses in the MMT spectra remain, the photometric colours are consistent with the spectral differences shown in Fig. 1. Contributing to the colour difference is not only the relatively redder continuum in HS 1216+5032B, but also the fact that the strong emission lines which fall into the *B* band are severely weakened by the BALs.

3 INFRARED SPECTRA

Near-IR spectra of HS 1216+5032 were obtained on UT 2003 March 20 and UT 2003 April 04 through the service programme at the United

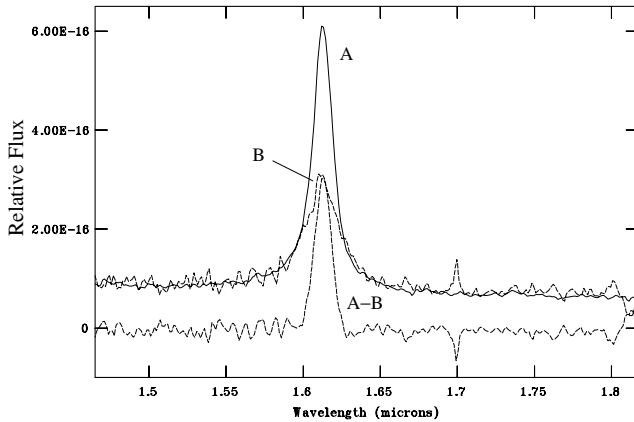


Figure 2. The H -band UKIRT spectrum of HS 1216+5032A. The next lowest spectrum is that of HS 1216+5032B, scaled upward by a constant factor of 4, after which the continuum shape and broad $H\alpha$ line wings of the two components are identical. At the bottom is the residual spectrum, which shows the strong narrow line emission absent in HS 1216+5032A.

Kingdom Infrared Telescope Facility (UKIRT) on Mauna Kea, using CGS4 with a 1.2-arcsec slit on to the 40 l mm^{-1} grating. The H -band spectra were taken in first order, centred at $1.6 \mu\text{m}$, with the B2 order separating filter ($> 1.43 \mu\text{m}$), while the J -band spectra were obtained in second order centred at $1.18 \mu\text{m}$, with the B1 filter ($> 0.99 \mu\text{m}$). Total exposure times for the spectra are 80 min in the J band and 48 min in the H band from each night. We used the two-dimensional (2D) spectra produced by the ORAC-DR pipeline (Economou et al. 2001). Our extraction and analysis uses standard procedures in the IRAF⁵ software package. The spectra have dispersions of 12 and $24 \text{ \AA pixel}^{-1}$ at J and H , respectively, or resolutions of about 600 and 900 km s^{-1} . To remove atmospheric absorption features, we obtained the spectrum of the F7V star BS 4761. We divided the stellar spectrum into the quasar spectrum, after each had been wavelength calibrated and normalized to the same integration time. To flux calibrate, we multiplied the resulting quotient by a blackbody spectrum having an effective temperature of 6250 K and normalized to the $V = 6.21$ magnitude of BS 4761. Given that the slit may not have been perfectly aligned on both components, we eschew detailed study of the continuum, and here concern ourselves only with relative line profiles.

In Fig. 2 we show the H -band UKIRT spectrum of HS 1216+5032A, along with that of HS 1216+5032B, scaled upward by a constant factor of 4. The continuum shape and broad $H\alpha$ line wings of the two components are identical. The redshifts we measure are $z_A = 1.4569 \pm 0.0006$ and $z_B = 1.4556 \pm 0.0015$, which is consistent with no significant velocity difference. The remaining equivalent widths are $W_\lambda = 630$ and $W_\lambda = 350 \text{ \AA}$ respectively (with errors of $\pm 50 \text{ \AA}$ dominated by choice of continuum placement). A strong narrow emission-line component in HS 1216+5032A is effectively absent in HS 1216+5032B, as can be seen from the residual spectrum at the bottom.

The lack of a strong narrow $H\alpha$ component in HS 1216+5032B is consistent with the fact that BALQSOs are known to have reduced narrow-line emission (Turnshek et al. 1997). More generally, X-ray weak quasars such as BALQSOs have relatively weaker nar-

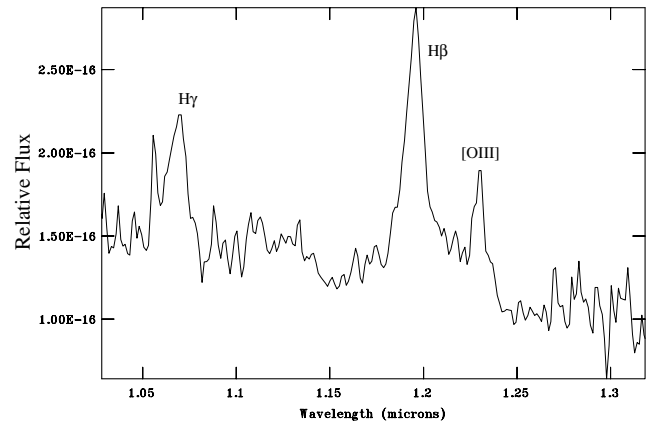


Figure 3. The J -band UKIRT spectrum of HS 1216+5032A. $H\beta$ and $[\text{O III}]\lambda 5007$ are clearly visible at 1.196 and $1.230 \mu\text{m}$ respectively. $H\gamma$ can be seen at $1.069 \mu\text{m}$. We derive a redshift of 1.456 from $[\text{O III}]\lambda 5007$. The J spectrum of HS 1216+5032B had insufficient S/N to detect emission lines.

row components to their emission lines (Green 1998). This has been proposed to be due to absorbers blocking the ionizing flux from reaching the larger narrow-line region (NLR). If the NLR is spatially extended (over several hundred pc; i.e. Kraemer & Crenshaw 2000), then small sightline differences should cause little change to total NLR flux. These differing $H\alpha$ profiles thus strongly discourage the lens hypothesis.

Fig. 3 shows the J -band UKIRT spectrum of HS 1216+5032A. For HS 1216+5032A, we derive a redshift of 1.456 from $[\text{O III}]\lambda 5007$ and $[\text{O III}]\lambda 4959$. The J -band spectra of HS 1216+5032B from UT 2003 March 20 had insufficient signal-to-noise ratio (S/N) to detect any emission lines. We tried again with longer exposures on UT 2003 April 20, but with only marginal improvement.

4 RADIO PROPERTIES

4.1 FIRST data

We searched for catalogued radio sources within 20 arcsec of HS 1216+5032A in the 20-cm VLA survey for FIRST. A source in the FIRST catalogue at $12^{\text{h}} 18^{\text{m}} 40^{\text{s}}.462 + 50^{\circ} 15' 43''.30$ is just 0.5 arcsec from the United States Naval Observatory B1.0 (USNO-B1.0; Monet et al. 2003) optical catalogue position of HS 1216+5032B.⁶ A sequence of tiled 1-arcmin images of the field in photographic B and R optical bands [Digitized Sky Survey (DSS) scans of the Second Palomar Observatory Sky Survey (POSS-II)], J , H and K near-IR bands [Two-Micron All-Sky Survey (2MASS)] and 20-cm radio bands (VLA FIRST) are shown in Fig. 4. The integrated radio flux of HS 1216+5032B is $3.92 \pm 0.143 \text{ mJy}$. This is identical to the peak flux in the beam, indicating that it is consistent with a point source at the ~ 5 arcsec spatial resolution of the FIRST. This flux corresponds at $z = 1.455$ to a (log) radio luminosity of $32.53 \text{ erg s}^{-1} \text{ Hz}^{-1}$. In contrast, no source is catalogued at the position of HS 1216+5032A, nor is one evident in the image. The rms of the

⁶ Source positions derived from FIRST images have an error of 0.5 arcsec rms for the weakest discernible point sources ($\sim 0.75 \text{ mJy}$) and substantially smaller uncertainties for brighter sources. McMahon et al. (2002) report FIRST positional uncertainties of < 1 arcsec (radius of 90 per cent confidence). The quoted position errors for the USNOB1.0 sources are about 0.1 arcsec.

⁵ IRAF is distributed by the National Optical Astronomy Observatory, which is operated by the Association of Universities for Research in Astronomy, Inc., under cooperative agreement with the National Science Foundation.

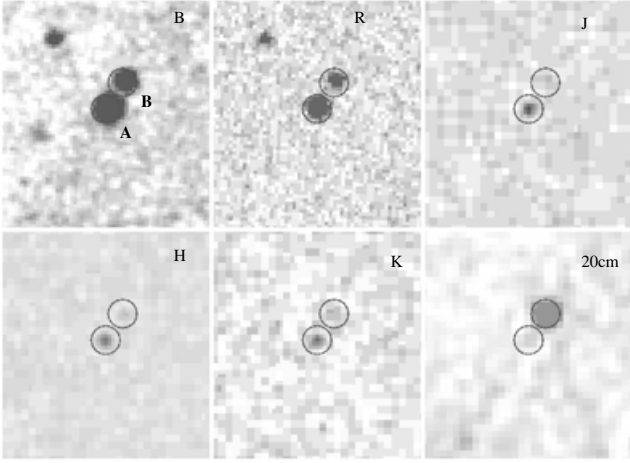


Figure 4. A mosaic of multiwavelength images of the HS 1216+5032 field gathered from the web. Each image is 1 arcmin on a side, with 4-arcsec diameter circles marking the USNO-B1.0 positions for the two components. The flux ratios in the DSSII *B* and *R* images, and those in the 2MASS *J*-, *H*- and *K*-band images are all roughly consistent with HS 1216+5032A, being brighter by a factor of 5–6. In the FIRST 20-cm (1.4 GHz) image, HS 1216+5032B is at least five times brighter.

background in the vicinity of HS 1216+5032 is 0.16 mJy, so that a 5σ upper limit for point source detection corresponds to 0.8 mJy, or $\log L_R < 31.83 \text{ erg s}^{-1} \text{ Hz}^{-1}$.

4.2 Radio-loudness differences

Combining optical with radio fluxes, we can constrain the radio-loudness $\log R$, which is the log ratio of the emitted monochromatic luminosity at 1.4 GHz and 4410 Å, $\log R \equiv \log(L_{1.4\text{GHz}}/L_{4410\text{Å}})$. To the observed *B* mag from Section 2, we apply a correction for extinction.⁷ We assume an intrinsic optical continuum $f_\nu \propto \nu^{-0.5}$, with specific optical normalization from Marshall et al. (1984).

We derive $\log R = 1.74$, with a conservative error estimate of ± 0.4 .⁸ A radio-loudness parameter greater than unity is typically the criterion for a radio-loud classification, and HS 1216+5032B surely qualifies.⁹ This marks HS 1216+5032B as one of a handful of bona fide radio-loud BALQSOs. Although BALQSOs were originally thought to be radio quiet as a rule (Stocke et al. 1992), by now more than 50 BAL quasars have been identified via radio selection, primarily from the FIRST Bright Quasar Survey (FBQS; Becker et al. 2000; Menou et al. 2001).

The limit we derive for HS 1216+5032A is $\log R < 0.20$, so the radio-loudness difference between A and B is significant at $>3\sigma$.

5 DISCUSSION

5.1 No hope for the lens hypothesis

As we mention in Section 2, variability or sightline differences might conceivably explain some of the large optical spectral and

⁷ We use $E(B-V) = 0.0184$ mag from the maps of Schlegel, Finkbeiner & Davis (1998), and assume an $R_V = 3.1$ absorbing medium, with $A(\lambda)/A(B)$ from Cardelli, Clayton, & Mathis (1989)

⁸ This error estimate allows for the worst-case combination of $1-\sigma$ photometric errors with errors ± 0.2 in the assumed continuum slopes.

⁹ A different definition of radio loudness, which divides QSOs into two populations at a radio luminosity of about $10^{25} \text{ W Hz}^{-1}$, does not affect any of the results we present here.

colour differences seen between the two image components of HS 1216+5032. Could sightline differences or variability explain the differing radio fluxes?

We first examine the properties of known lenses and lens candidates to see if radio flux ratios of ~ 5 are common. The Cosmic Lens All-Sky Survey (CLASS) requires a double detection and a component flux density ratio of < 10 as a selection criterion (Browne et al. 2003). Four out of seven pairs in the CLASS statistically well-defined sample have flux ratios above 5. In a lens scenario, we may choose to assume that the optical/near-IR flux ratio of ~ 5 represents the ratio of the magnification factors due to the lens. The difference in radio flux in the opposite sense by another factor of ≥ 5 requires a factor of ~ 25 intrinsic radio flux difference to be due to the 9.1-arcsec sightline shift. If the jet is Doppler boosted, the observed flux f_ν is related to the source rest-frame flux f'_ν via

$$f_\nu = \left(\frac{D}{1+z} \right)^{3+\alpha} f'_\nu$$

where α is the radio spectral index and D is the Doppler boosting factor

$$D = \frac{1}{\gamma(1 - \beta \cos \theta)}$$

(Rybicki & Lightman 1979). Even assuming a very fast jet ($\beta = 0.9$), for any line-of-sight angle θ to the jet direction, the maximum change in Doppler boosting achieved by a 9-arcsec change in θ is a factor of about 2×10^{-4} , so nowhere near capable of explaining the observed radio flux ratio.

Some radio-quiet or radio-intermediate objects flare by factors of ~ 30 at high frequencies (i.e. III Zw2 at 22 GHz; Brunthaler et al. 2003). Among flat spectrum (typically core-dominated) quasars (~ 40 per cent) variability of radio sources on scales of 1–5 yr is common. The spectral and variability characteristics of such quasars are very similar (Valtaoja et al. 1992) to those of BL Lacs. However, variability rarely exceeds about 20 per cent – at 151 MHz (Riley 1993) or 1.4 GHz (Rys & Machalski 1990) – and few variations of $>5\times$ are known. Therefore, variability combined with time delays is very unlikely to account for the differing radio loudness of HS 1216+5032A and B.

5.2 The interaction/merger hypothesis

Because the number of WSQPs is $\sim 100\times$ that expected from simple extrapolations of the quasar–quasar correlation function, galaxy interactions may be important in creating binary quasars (Kochanek, Falco & Munoz 1999; Mortlock, Webster & Francis 1999) and can be used as a tool to study the triggering of nuclear activity in galaxies (Osterbrock 1993).

Because it appears most convincingly from the radio-loudness differences that HS 1216+5032 is not lensed, the two quasars are separated by at least their projected separation of $\sim 65 h_{70}$ kpc. HS 1216+5032 could represent a high- z example of interaction-triggered but as-yet unmerged luminous AGN. Approach velocities less than the internal host galaxy velocities induce significant angular momentum loss (Fang & Saslaw 1997) and merging over 6–10 crossing times. Assuming an encounter space velocity of 500 km s^{-1} and 50-kpc separation implies that the last encounter occurred ~ 100 Myr ago in the QSO rest frame.

This would support the view of quasar activity as a short active phase of supermassive black holes accreting at rate $\dot{M} \sim 1-100 M_\odot \text{ yr}^{-1}$ (Rees 1984). Cavaliere & Vittorini (2000), Menci et al. (2003) and others have proposed that earlier than $z \sim 3$, gas-rich

protogalaxies grow by merging, simultaneously inducing growth of central holes accreting at their full Eddington rates. More recently (for $z < 3$) the black holes are triggered by the encounters of a gas-rich host with its companions in a group, which destabilize the gas and induce accretion. These models link hierarchical structure formation, the observed evolution of the quasar luminosity function (space density peaking near $z \sim 3$), and the correlation between central black hole and bulge masses in nearby galaxies (Ferrarese & Merritt 2000; Gebhardt et al. 2000). Higher rates of interaction and triggered activity in close pairs must be demonstrated to verify the premises of these models.

The weak [O III] lines in the J -band spectrum of HS 1216+5032A suggest that it has similarities to HS 1216+5032B. A principal component analysis of low-redshift optical spectra reveals that the principal eigenvector of a quasar spectral sample (PC1, the linear combination of parameters that represents the largest variance in the sample spectra) links the strength of Fe II emission, [O III] emission, and $H\beta$ line asymmetry (Boroson & Green 1992). In a common interpretation, objects with weak [O III]/ $H\beta$ ratios have high Eddington ratios L/L_{Edd} . The second principal eigenvector (PC2), dominated by luminosity and its anticorrelation with the strength of He II $\lambda 4686$, is presumed to be driven by accretion rate \dot{M} . The J -band spectrum of HS 1216+5032A is clearly on the low PC1, low PC2 end (cf. fig. 2 of Boroson 2002), which is the region also inhabited by BALQSOs (their fig. 1). Only ~ 10 per cent of quasars inhabit this region of observational parameter space, which is proposed to map physically to high L/L_{Edd} and \dot{M} . Because HS 1216+5032 is not lensed, then these quasars probably have both high L and L/L_{Edd} in common, perhaps related to a common dense environment (i.e. a cluster) or to the ongoing effects of their interaction. While the current example is anecdotal, its properties should help guide directed searches for other examples.

6 SUMMARY

The HS 1216+5032 quasar pair, particularly with evidence for an intervening cluster potential, held out promise of being a dark lens system. We obtained improved optical (MMT) and IR (UKIRT) spectra of HS 1216+5032A and HS 1216+5032B, away from the strongest (UV) effects of BALs, and measured the emission lines, finding significant differences in the $H\alpha$ profiles. Optical B , V and R colours measured at the WIYN telescope confirm different continuum shapes.

From FIRST data, we confirm that HS 1216+5032B is radio loud, to a degree that we find is not plausibly explained in a lens + time-delay scenario by either variability or line-of-sight differences. The HS 1216+5032 pair is thus certainly a physical quasar binary rather than a lensed system. The system remains interesting because there are only a handful of bona fide radio-loud BALQSOs known to date, and because BALQSOs have been proposed to be high Eddington ratio accretors that are triggered by interactions.

ACKNOWLEDGMENTS

Thanks to Chris Kochanek, Dan Schwartz and Bryan Gaensler for useful comments, and to Deborah Freedman for attempting imaging for us at the F. L. Whipple Observatory (FLWO) 1.2-m on Mt Hopkins. We thank the referee, Paul Hewett, for advice and pruning. This work was supported by CXO grant GO2-3132X and NASA grant NAS8-39073. PJG and TLA gratefully acknowledge support through NASA Contract NAS8-39073 (CXC).

The IR spectra were obtained as part of the UKIRT Service Programme. UKIRT is operated by the Joint Astronomy Centre on behalf of the UK Particle Physics and Astronomy Research Council. ORAC-DR, the UKIRT data reduction pipeline, was developed at the Joint Astronomy Centre by Frossie Economou and Tim Jenness in collaboration with the UK Astronomy Technology Centre.

Optical spectra were obtained by WRB at the MMT Observatory, a joint facility of the Smithsonian Institution and the University of Arizona. WIYN photometry was obtained at Kitt Peak, part of the National Optical Astronomy Observatory, operated by the Association of Universities for Research in Astronomy, Inc., under cooperative agreement with the National Science Foundation.

The DSS was produced at the Space Telescope Science Institute under US Government grant NAGW-2166. The images of these surveys are based on photographic data obtained using the Oschin Schmidt Telescope on Palomar Mountain and the UK Schmidt Telescope. The plates were processed into the present compressed digital form with the permission of these institutions. The POSS-II was made by the California Institute of Technology with funds from the National Science Foundation, the National Aeronautics and Space Administration, the National Geographic Society, the Sloan Foundation, the Samuel Oschin Foundation, and the Eastman Kodak Corporation.

This research has made use of the USNOFS Image and Catalogue Archive operated by the USNO, Flagstaff Station (<http://www.nofs.navy.mil/data/fchpix/>).

REFERENCES

- Aldcroft T. L., Green P. J., 2003, *ApJ*, 592, 710
 Barlow T. A., Junkkarinen V. T., Burbidge E. M., Weymann R. J., Morris S. L., Korista K. T., 1992, *ApJ*, 397, 81
 Becker R. H., White R. L., Gregg M. D., Brotherton M. S., Laurent-Muehleisen S. A., Arav N., 2000, *ApJ*, 538, 72
 Boroson T. A., 2002, *ApJ*, 565, 78
 Boroson T. A., Green R. F., 1992, *ApJS*, 80, 109
 Browne I. W. A. et al., 2003, *MNRAS*, 341, 13
 Brunthaler A., Falcke H., Bower G. C., Aller M. F., Aller H. D., Teräsranta H., Krichbaum T. P., 2003, *PASA*, 20, 126
 Cardelli J. A., Clayton G. C., Mathis J. S., 1989, *ApJ*, 345, 245
 Cavaliere A., Vittorini V., 2000, *ApJ*, 543, 599
 Chelouche D., 2003, *ApJ*, 596, L43
 Economou F., Jenness T., Cavanagh B., Wright G. S., Bridger A. B., Kerr T. H., Hirst P., Adamson A. J., 2001, in Harnden F. R. Jr., Primini F. A., Payne H. E., eds, *ASP Conf. Ser. Vol. 238, Astronomical Data Analysis and Systems X*. Astron. Soc. Pac., San Francisco, p. 314
 Falco E. E. et al., 1999, *ApJ*, 523, 617
 Fang F., Saslaw W. C., 1997, *ApJ*, 476, 534
 Ferrarese L., Merritt D., 2000, *ApJ*, 539, L9
 Gebhardt K. et al., 2000, *ApJ*, 539, L13
 Green P. J., 1998, *ApJ*, 498, 170
 Green P. J. et al., 2002, *ApJ*, 571, 721
 Hagen H.-J., Hopp U., Engels D., Reimers D., 1996, *A&A*, 308, L25
 Hall P. B. et al., 2002, *ApJS*, 141, 267
 Keeton C. R. et al., 2000, *ApJ*, 542, 74
 Kochanek C. S., Falco E., Munoz J. A., 1999, *ApJ*, 510, 590
 Kraemer S. B., Crenshaw D. M., 2000, *ApJ*, 544, 763
 Lewis G. F., Ibata R. A., Ellison S. L., Aracil B., Petitjean P., Pettini M., Srianand R., 2002, *MNRAS*, 334, L7
 Lopez S., Hagen H.-J., Reimers D., 2000, *A&A*, 357, 37
 Marshall H. L., Avni Y., Braccetti A., Huchra J. P., Tananbaum H., Zamorani G., Zitelli V., 1984, *ApJ*, 283, 50
 McMahon R. G., White R. L., Helfand D. J., Becker R. H., 2002, *ApJS*, 143,

- Menci N., Cavaliere A., Fontana A., Giallongo E., Poli F., Vittorini V., 2003, *ApJ*, 587, L63
- Menou K. et al., 2001, *ApJ*, 561, 645
- Monet D. G. et al., 2003, *AJ*, 125, 984
- Mortlock D. J., Webster R. L., Francis P. J., 1999, *MNRAS*, 309, 836
- Muñoz J. A. et al., 2001, *ApJ*, 546, 769
- Osterbrock D. E., 1993, *ApJ*, 404, 551
- Peng C. Y. et al., 1999, *ApJ*, 524, 572
- Rees M. J., 1984, *ARA&A*, 22, 471
- Reichard T. A. et al., 2003, *AJ*, 125, 1711
- Riley J. M., 1993, *MNRAS*, 260, 893
- Rybicki G. B., Lightman A. P., 1979, *Radiative Processes in Astrophysics*. Wiley, New York
- Rys S., Machalski, J., 1990, *A&A*, 236, 15
- Schlegel D. J., Finkbeiner D. P., Davis M., 1998, *AJ*, 500, 523
- Schneider P., Ehlers J., Falco E. E., 1992, *Gravitational Lenses*. Springer-Verlag, Berlin
- Stoche J. T., Morris S. L., Weymann R. J., Foltz C. B., 1992, *ApJ*, 396, 487
- Turnshek D. A., Monier E. M., Sirola C. J., Espey B. R., 1997, *ApJ*, 476, 40
- Weymann R. J., Morris S. L., Foltz C. B., Hewett P. C., 1991, *ApJ*, 373, 23
- Valtaoja E., Terasranta H., Urpo S., Nesterov N. S., Lainela M., Valtonen M., 1992, *A&A*, 254, 80

This paper has been typeset from a \TeX/L\TeX file prepared by the author.